

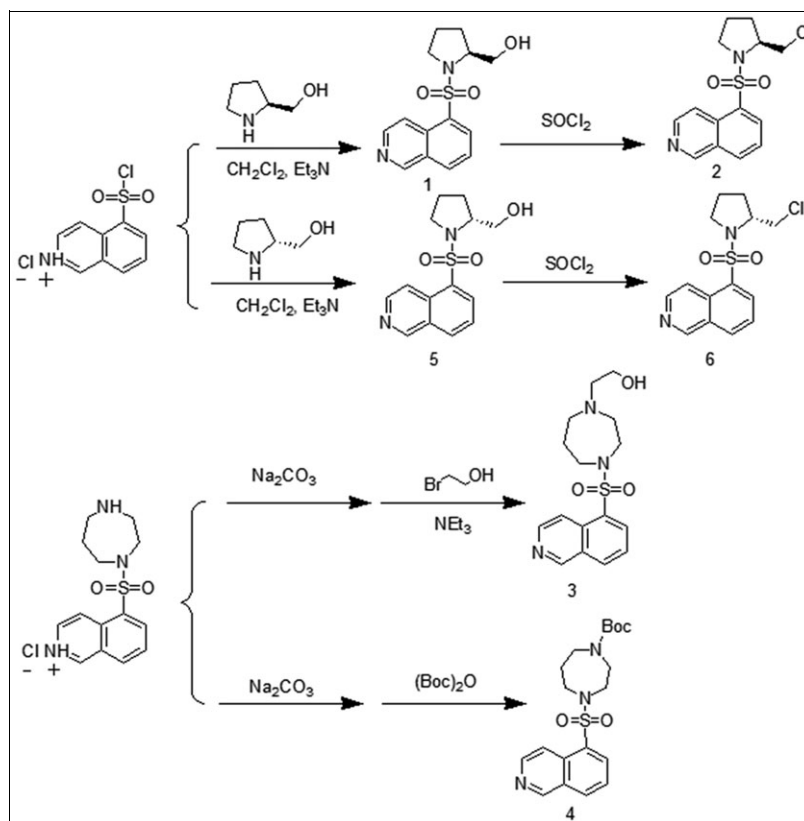
Hang Li,<sup>a\*</sup>  Xueyong Zhou,<sup>a</sup> Hang Ye,<sup>b</sup> Xi Sun,<sup>a</sup> and Pingping Zhang<sup>a</sup><sup>a</sup>College of Food Science and Bioengineering, Tianjin Agricultural University, Tianjin 300072, People's Republic of China<sup>b</sup>R&D of Danfoss (Tianjin) Ltd., Tianjin 301700, People's Republic of China

\*E-mail: lihang18888@163.com

Received July 31, 2018

DOI 10.1002/jhet.3403

Published online 00 Month 2018 in Wiley Online Library (wileyonlinelibrary.com).



In our previous work, (*S*)-6*H*-1-(5-isoquinolinesulfonyl)-2-hydroxymethyl-1-pyrrolidine and (*S*)-6*H*-1-(5-isoquinolinesulfonyl)-2-chloromethyl-1-pyrrolidine displayed potent inhibitory activity. Therefore, with these two substances as lead compounds, we designed and synthesized their enantiomers to reveal the inhibitory effects of chirality on Rho kinase. It is found that their enantiomers exhibited much better Rho kinase inhibitory activity and strongly promoted synapse formation. Experimental autoimmune encephalomyelitis is a murine autoimmune disease used to study multiple sclerosis. With added antigens, the changes from C57BL/6 mice's limbs and tail was observed and scored by clinical evaluation. The synthetic compounds may simultaneously reduce symptoms of experimental autoimmune encephalomyelitis and inhibit inflammatory infiltration of the central nervous system. Thus, these compounds may be potential candidates for inhibition of Rho kinase and should be considered for further experimental study in relation to multiple sclerosis.

*J. Heterocyclic Chem.*, **00**, 00 (2018).

## INTRODUCTION

Experimental autoimmune encephalomyelitis (EAE) has become recognized as a classic model for studying multiple sclerosis (MS), and its clinical and histopathological changes closely resemble the disease. MS is a central nervous system (CNS) inflammatory

autoimmune disease, with the most prominent physiological characteristics being axonal damage and demyelination. The clinical manifestations are recurrent and associated with extremely high morbidity [1]. Activation of Rho kinase, also known as Rho-associated coiled-coil forming protein serine kinase (ROCK) produces closely related pathophysiological effects such as

vasoconstriction, inflammation, and cell apoptosis [2–4]. Fasudil hydrochloride is a ROCK inhibitor commonly used for clinical purposes as well as being a focus for ongoing research. Fasudil effectively reduces the onset and clinical symptoms of EAE and also decreases the peripheral inflammatory response and improves the CNS microenvironment. Over the past two decades, Rho kinase inhibitors have been studied intensively [5–9]. Chen *et al.* reported that fasudil promoted axonal growth, inhibited myelin loss, reduced accumulation of inflammatory cells, decreased the release of inflammatory cytokines, and improved the CNS function [10]. Yu *et al.* showed that fasudil prevented synaptic damage and promoted synapse formation by increasing EAE mouse CNS neurotrophic factor and reducing the CNS inflammatory microenvironment [11]. Fasudil combined with bone marrow-derived neural stem cells promoted expression of neurotrophic factors and improved the CNS microenvironment. Therefore, fasudil plays a positive role in neural restoration and regeneration through synergistic and superimposed effects [12].

In our previous work, we found that (*S*)-6*H*-1-(5-isoquinolinesulfonyl)-2-hydroxymethyl-1-pyrrolidine (compound **1**) and (*S*)-6*H*-1-(5-isoquinolinesulfonyl)-2-chloromethyl-1-pyrrolidine (compound **2**) displayed excellent Rho kinase inhibitory activity and also promoted synapse formation (Fig. 1) [13]. Encouraged by this result, the enantiomers of compounds **1** and **2** were synthesized in our laboratory and named compounds **5** and **6**. Compound **3**, with a hydroxyethyl group at the nitrogen atom of homopiperazine, provided a new binding site. To be clear that modification of the hydroxyl group produced a good binding site, we designed compound **4** to block hydrogen bond formation at region D [13,5–7]. The enantiomers (*R*)-6*H*-1-(5-isoquinolinesulfonyl)-2-hydroxymethyl-1-pyrrolidine and (*R*)-6*H*-1-(5-isoquinolinesulfonyl)-2-chloromethyl-1-pyrrolidine exhibited much better Rho kinase inhibitory activity and strongly promoted synapse formation than fasudil. The effects of these synthesized compounds on Rho kinase inhibitory activity and synapse formation were systematically evaluated. We also examined the therapeutic effect of these synthetic compounds, administered *via* the nasal cavity, on development of EAE in mice. We aimed to develop new Rho kinase

inhibitors with improved Rho kinase inhibitor activity, better synapse formation, and no obvious inflammatory infiltration.

## CHEMISTRY

With fasudil as the lead compound, six analogues were designed. Their synthesis is outlined in Scheme 1. Compound **1** was obtained by treatment of isoquinoline sulfonyl chloride with L-prolinol in methylene dichloride, with a 95% yield. The resulting compound was treated with thionyl chloride to produce compound **2**, with a 75% yield. Compound **3** was similarly obtained by typical N-alkylation of fasudil with corresponding halides. Compound **4** was synthesized, Boc-protected fasudil in 97% yield. Using a similar synthetic procedure, compound **5** was obtained from D-prolinol, with a 95% yield. Compound **5** was treated with SOCl<sub>2</sub> to produce compound **6** in 75% yield.

The biological activities of these compounds were evaluated systematically. The obtained products were fully characterized by <sup>1</sup>H and <sup>13</sup>C NMR spectroscopy, IR spectroscopy, and high-resolution mass spectroscopy (HRMS). The biological activities assessed included Rho kinase inhibition, synapse formation, and EAE clinical symptoms.

## RESULTS AND DISCUSSION

Considering the chiral structure might play an important role for the improvement of biological activity, compounds **1–6** were evaluated for their Rho kinase inhibitory activity, synapse formation, and EAE clinical symptoms as shown in the following figures.

**ROCK kinase inhibitor activity.** Results are shown in Figure 2. Compounds **1**, **2**, **5**, and **6** had excellent inhibitory abilities. The hydroxy group within compound **2** was important for the formation of the hydrogen bond and helped to improve Rho kinase inhibitory activity. Compounds **2** and **6** existing chlorine also gave rise to excellent results. Compound **3** has lesser inhibitory effects, perhaps due to steric hindrance by the six-membered ring. It is already established that the hydroxylated fasudil exhibited much higher Rho kinase inhibitory activity than fasudil *in vivo*. However, compound **4**, as the hydroxyl fasudil intermediate, did not have good Rho kinase inhibitory activity. Compounds **1**, **2**, **5**, and **6**, as two pairs of chiral compounds, improved Rho kinase inhibitory activity. These results suggested that the hydroxyl group and the chloro heteroatom might play an important role in the inhibition of Rho kinase activity.

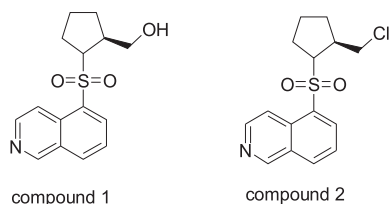


**Figure 1.** The chemical structure of compounds **1** and **2**.

**Scheme 1.** Synthesis of compounds 1–6: (a) saturated sodium carbonate solution, 0.5 h; (b)  $\text{CH}_2\text{Cl}_2$ , 0–5°C, 2 h; (c) 40°C, 2 h; (d) room temperature 30 h; and (e) room temperature 1 h. Yields for compounds 1–6: 95%, 75%, 65%, 97%, 95%, and 75%, respectively. [Color figure can be viewed at [wileyonlinelibrary.com](http://wileyonlinelibrary.com)]

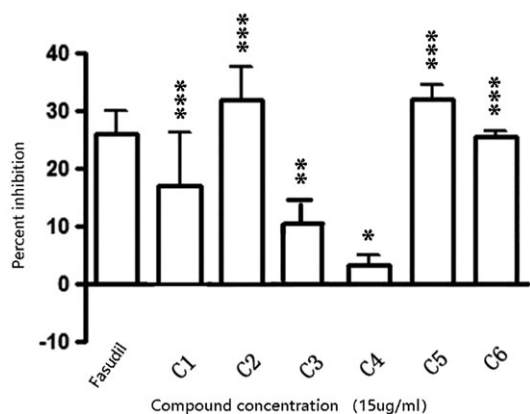
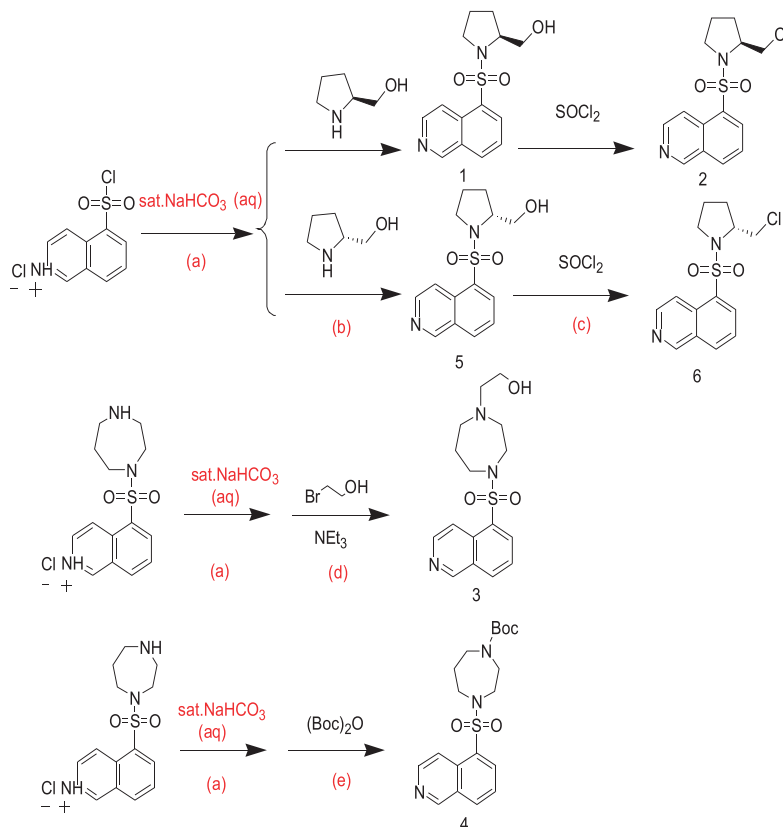


**Figure 2.** ROCK kinase inhibitor activity. BV-2 microglia were cultured in the presence of fasudil and compounds (C) 1–6 (10  $\mu\text{g/mL}$ ) for 24 h. ROCK activity was measured by ROCK assay kit. Quantitative value represents means  $\pm$  standard deviation from three independent experiments with similar results. \* $p < 0.05$ , \*\* $p < 0.01$ , \*\*\* $p < 0.001$ .

**Determination of synapse formation.** Findings regarding synapse formation in primary neuronal cells and BV-2 microglia cells are presented in Figure 3. As

shown in Figure 3(a), compound 5 more effectively enhanced the synapse formation of primary neurons than compound 1, while compound 2 was better than its enantiomer, compound 6. Therefore, chiral inhibitors exhibited similar activity on primary neuron synapse formation. As shown in Figure 3(b) and consistent with the aforementioned findings, enhancement of BV-2 microglial cell synapse formation was attributed to the deactivation of Rho kinase. It is worth noting that compounds 5 and 6 were better than fasudil in BV-2 microglial cell synapse formation.

The longest synapses were found in the presence of compound 2, while compound 5 took second place in the enhancement of synapse formation as shown in Figure 3 (c). This result further demonstrated that the chlorine atom in compound 5 is an important binding site with region D of Rho kinase causing Rho kinase inhibition and enhanced synapse formation. Furthermore, longer synapses were observed with compound 5 than compound 1 and with compound 2 compared with compound 6. This indicated that inhibitor chirality plays an important role in Rho kinase inhibition. We understand Rho kinase to be closely related to synapse

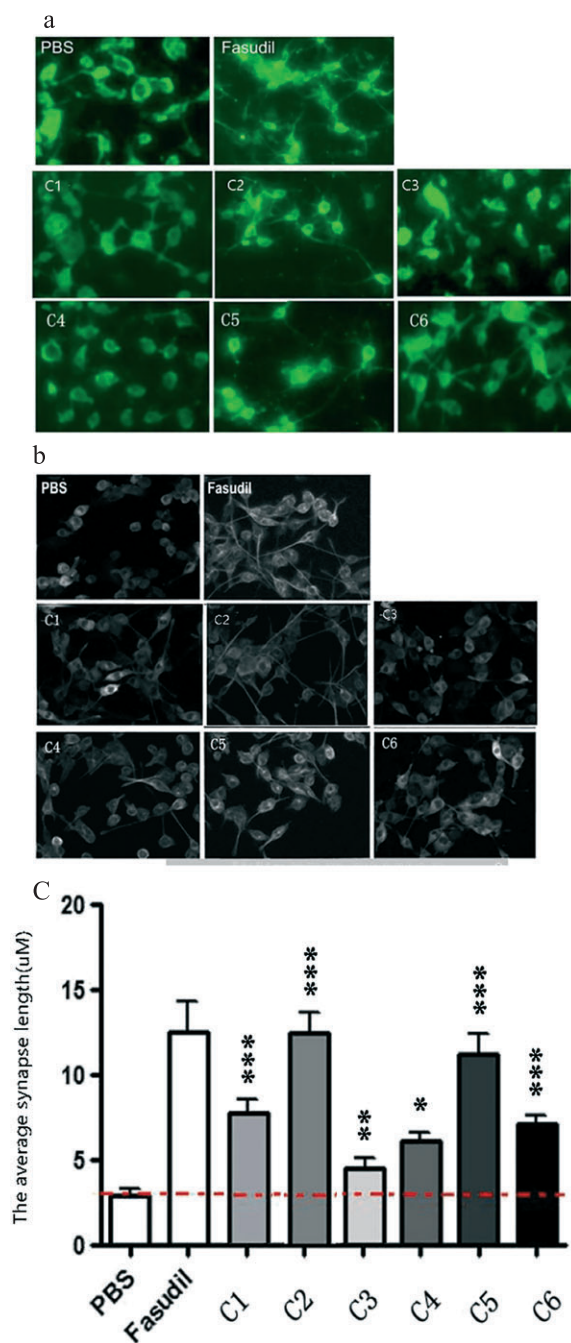


**Figure 3.** Determination of synaptic formation: (a) primary neurons, (b) BV-2 microglia, and (c) synapse length by BV-2 microglia. Microglia and primary neurons were cultured in the presence of fasudil and compounds (C) 1–6 (15 g/mL) for 24 h. The densities of dendritic spines on BV-2 cells were observed under phase contrast microscope. Primary neurons were stained with anti-MAP-2 antibody, and the synaptic formation of neurons was determined under fluorescence microscopy. Microphotographs are representative of three independent experiments with similar results. \* $p < 0.05$ , \*\* $p < 0.01$ , \*\*\* $p < 0.001$ . PBS, phosphate-buffered saline. [Color figure can be viewed at [wileyonlinelibrary.com](http://wileyonlinelibrary.com)]

formation. As Rho kinase activation has a key role in axonal growth inhibition, blockade of Rho kinase can promote axonal regeneration [14–16]. The Rho kinase inhibitor, Y-27632, also enhanced retina ganglion cell axon growth on glial scar tissue [17,18]. In a streptozotocin-treated rat model, learning and memory were impaired. However, fasudil administration improved synaptic transmission in the CA1 region of the hippocampus, as well as increasing synaptophysin expression and improving learning and memory [19]. These findings indicate that Rho-ROCK is an appropriate target to promote synapse formation and to improve learning and memory ability. Compounds **5** and **6**, as the novel ROCK inhibitors, showed better synapse formation than fasudil, providing a therapeutic potential against injuries to the human, such as spinal cord injuries, stroke, and neurodegenerative disorders.

**Determination of experimental autoimmune encephalomyelitis clinical symptoms.** Over the past few years, nasal drug administration has drawn wide attention for therapeutics. Several studies have shown that drugs can be effective when administered through the olfactory mucosa epithelium. This route bypasses the blood–brain barrier, enabling drug to enter the cerebrospinal fluid and directly diffused into the CNS. The drug also enters the brain through indirect pathways such as *via* the blood or lymphatic systems, or the trigeminal and optic nerves [12]. Our experiment aimed to detect whether the clinical symptoms of EAE were reduced by nasal administration of the different compounds. In the experiment, fasudil was injected intraperitoneally into the positive control group. The clinical symptoms curve for the EAE model is shown: Compound **2** had the most ideal symptom relief following nasal cavity injection. Compounds **4** and **5** had no effect at all, whereas compound **3** was characterized by rapid and marked onset of symptom relief. Injecting fasudil and synthesized compounds by nasal administration, compound **1** had the better ideal symptom relief effect through nasal cavity injection. However, compound **6** worsened in the later stages of the disease. In the established EAE model, nasal administration of fasudil and compounds **1**, **2**, and **6** postponed EAE onset and alleviated its symptoms.

Figure 4(b) shows the performance of compounds **1–6** on the pathological process of cellular inflammatory infiltration in mouse brain slices. In EAE model mice, brain was infiltrated with a large number of aggregated inflammatory infiltrating CD68 positive cells. After treatment with the various compounds, a small number of infiltration cells were found in the brain of EAE model mice. However, with compound **4**, mouse brain had a large number of infiltrating cells. Therefore, fasudil and compounds **1**, **2**, **5**, and **6** significantly reduced CNS

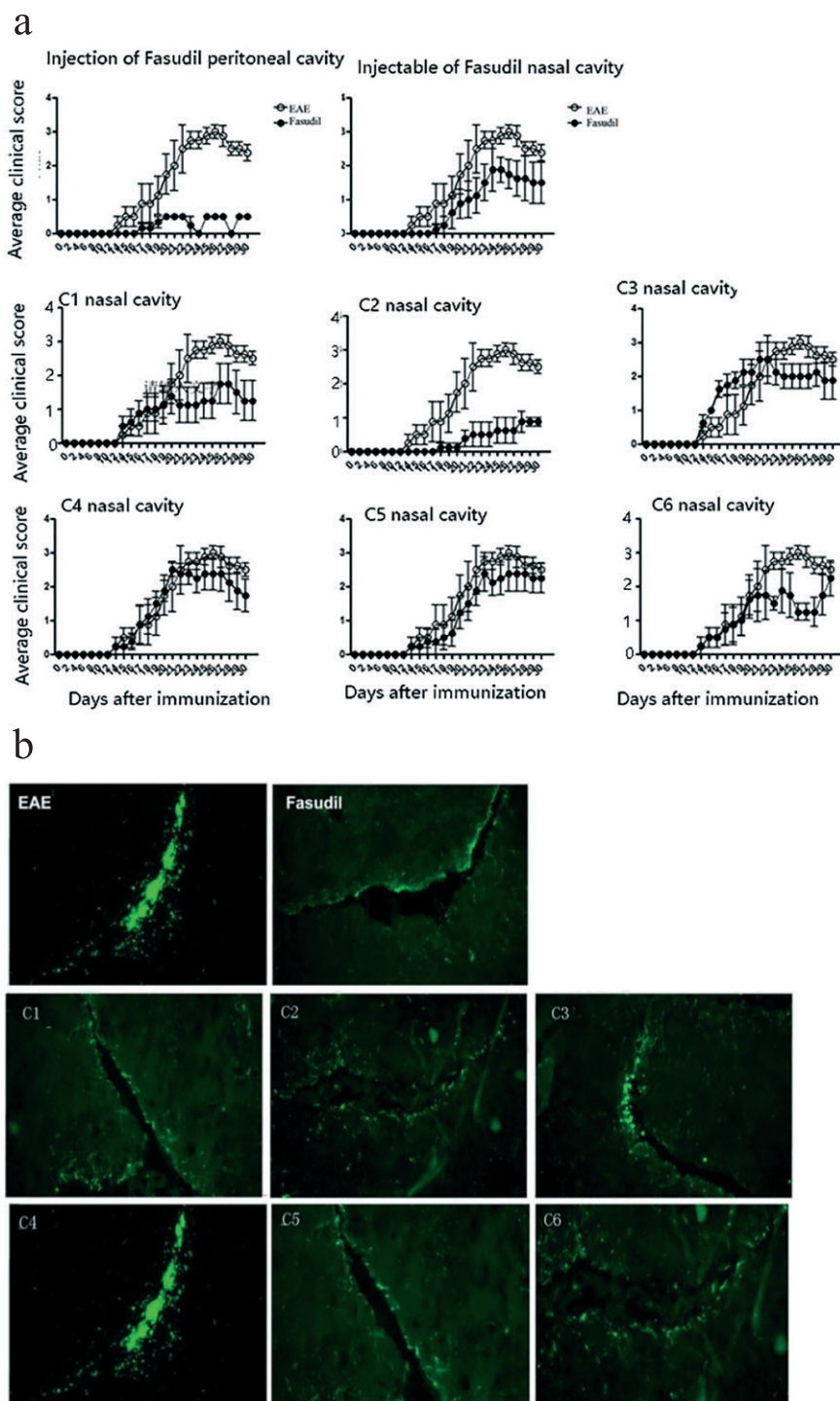


**Figure 4.** (a) The impact on clinical symptoms of experimental autoimmune encephalomyelitis (EAE) in the presence of fasudil and the synthesized compounds 1–6 (10  $\mu\text{g/mL}$ ) for 24 h. Criteria: 0 – no clinical symptom; 1 – tail tension disappears and slightly clumsy; 2 – unilateral hind limb atony that can be restored with passive turning over; 3 – bilateral hind limb paralysis with inability to recover autonomously after turning over but movement able to be stimulated; 4 – bilateral hind and fore limbs paralysis; and 5 – near-death or death. Between the two standards, the score is plus or minus 0.5. (b) The impact on inflammatory cell pathology. The examination of compounds 1–6 on inflammatory cell infiltration on mouse brain slices. A large number of inflammatory infiltrating CD68 positive cells invaded the brain of EAE model mice and was observed under an electron microscope. [Color figure can be viewed at [wileyonlinelibrary.com](http://wileyonlinelibrary.com)]

inflammatory infiltration, essentially in line with our observations regarding the clinical symptoms of EAE.

To our knowledge, the expression of ROCK kinase inhibitor is significantly upregulated in EAE mice, with symptoms of EAE improving with administration of fasudil. This may relate to the inhibition of ROCK-II and the decrease of inflammatory infiltration [20,21]; Zhang *et al.* reported that fasudil oral delays the onset of EAE, slows down EAE symptoms, reduces weight loss, and reduces EAE myelin loss and CNS inflammation infiltration. Fasudil oral has a good therapeutic effect and can significantly reduce the core of the CNS, which can significantly alleviate the loss of myelin and inflammatory lesions in the CNS [22]. Compounds **1**, **2**, and **6**, as the novel ROCK inhibitors, might provide a therapeutic potential against injuries to the human CNS.

## CONCLUSION

Compounds **1** and **2** displayed excellent Rho kinase inhibitory activity; we designed and synthesized their enantiomers to reveal the inhibitory effects of chirality on Rho kinase. It is found that their enantiomers also exhibited much better Rho kinase inhibitory activity and strongly promoted synapse formation than fasudil. Establishing the EAE model, after added antigens, the changes of limbs and tail were observed and scored by clinical evaluation. The synthetic compounds may simultaneously reduce symptoms of EAE and inhibit inflammatory infiltration of the CNS. Thus, compounds **1**, **2**, **5**, and **6** may be potential candidates for inhibition of Rho kinase and should be considered for further experimental study in relation to MS. Further studies on combination mode between inhibitors and Rho kinase are currently under way.

## EXPERIMENTAL

**General.** All the chemicals were purchased from Guangfu Technology Development Co., Ltd., Tianjin (China) and Chase Sun Pharmaceutical Co., Ltd., Tianjin (China) unless otherwise stated. All reagents were used as purchased from commercial suppliers without further purification. Solvents were dried and purified according to standard procedures before use. The course of reactions was monitored by thin-layer chromatography (silica gel GF254s); flash chromatography was performed using 200–300 mesh silica gel.  $^1\text{H}$  and  $^{13}\text{C}$  NMR spectra were recorded on INOVA400/600 Hz spectrometer with tetramethylsilane as an internal standard. HRMS was recorded on MicroOTOF-Q II (CycLex Co., Ltd, Nagano, Japan).

The synthesis of compounds **1** and **2** has been shown in our previous experiment [13], not repeated here.

**6H-1-(5-Isoquinolinesulfonyl)-4-( $\beta$ -hydroxy ethyl)-1,4-diazepine (compound 3).** Fasudil hydrochloride (1.00 g, 2.74 mmol) was slowly added to a saturated sodium bicarbonate solution (0.52 g, 4.93 mmol). The mixture kept its pH at a constant value (pH 5–6). This solution was stirred for 30 min and extracted with 20-mL  $\text{CH}_2\text{Cl}_2$ . Then, it was dried over anhydrous  $\text{MgSO}_4$ , followed by filtration and concentration. The residue dissolved in 20-mL  $\text{CH}_2\text{Cl}_2$  was dropwise added to triethylamine (0.33 g, 3.30 mmol). Then, 2-bromoethanol (0.90 g, 8.23 mmol) was added slowly to the mixture. The reaction was allowed to develop for 30 h at room temperature. And then, the organic layer was concentrated. The residue was purified by flash chromatography (ethyl acetate) to afford compound **3** (0.57 g, 65%) as a yellow oil.  $^1\text{H}$  NMR (500 MHz,  $\text{CDCl}_3$ )  $\delta$ : 1.81–1.86 (m, 2H), 2.61 (t,  $J_1 = 6.0$  Hz,  $J_2 = 6.0$  Hz, 2H), 2.65–2.68 (m, 4H), 3.47–3.51 (m, 4H), 3.59 (m, 2H), 7.65–7.68 (m, 1H), 8.17 (d,  $J = 9.0$  Hz, 1H), 8.34 (d,  $J = 9.0$  Hz, 1H), 8.45 (d,  $J = 6.0$  Hz, 1H), 8.66 (d,  $J = 6.0$  Hz, 1H), 9.33 (s, 1H).  $^{13}\text{C}$  NMR (125 MHz,  $\text{CDCl}_3$ )  $\delta$ : 8.50, 18.50, 45.67, 45.76, 55.19, 55.97, 57.69, 116.88, 126.62, 128.84, 130.60, 131.69, 132.79, 133.01, 134.02, 145.02, 153.55. HRMS (ESI), Calcd  $\text{C}_{16}\text{H}_{21}\text{N}_3\text{O}_3\text{S}$ :  $[\text{M} + \text{H}] + m/z$ : 336.1374. Found: 336.1376. IR (KBr  $\text{cm}^{-1}$ ): 3489, 3419, 2974, 2737, 1366, 1147, 1074, 678, 570.

**4-(Isoquine-5-sulfonyl)-[1,4]diazepane-1-carboxylic acid tert-butyl ester (compound 4).** Fasudil hydrochloride (5.00 g, 14 mmol) was slowly added to a saturated sodium bicarbonate solution (2.62 g, 24 mmol). The mixture kept its pH at a constant value (pH 5–6). The mixture was stirred 0.5 h and extracted with 50-mL  $\text{CH}_2\text{Cl}_2$  for three times. The organic layers were dried and concentrated. The residue dissolved in 50-mL  $\text{CH}_2\text{Cl}_2$  was added dropwise to the flask containing Di-tert-butylpyrocarbonate (4.49 g, 20.6 mmol) and triethylamine (1.39 g, 13.7 mmol). The mixture was stirred at 0–5°C for 2 h. After dried and concentrated, the residue was purified to afford compound **4** (5.25 g, 97%) as a yellow oil.  $^1\text{H}$  NMR (400 MHz,  $\text{CDCl}_3$ )  $\delta$ : 8.84 (s, 1H), 8.53 (d,  $J = 10$  Hz, 1H), 8.25 (d,  $J = 5$  Hz, 1H), 8.05–8.10 (m, 1H), 7.91 (d,  $J = 10$  Hz, 1H), 7.67 (d,  $J = 15$  Hz, 1H), 3.49–3.58 (m, 4H), 3.35–3.43 (m, 4H), 1.43 (s, 9H).  $^{13}\text{C}$  NMR (100 MHz,  $\text{CD}_3\text{OD}$ )  $\delta$ : 27.12, 28.76, 40.10, 42.25, 43.92, 47.07, 70.97, 120.27, 127.35, 127.10, 130.57, 132.54, 137.17, .51, 136.13, 142.71, 152.20, 155.79. HRMS (ESI), Calcd  $\text{C}_{19}\text{H}_{25}\text{N}_3\text{O}_4\text{S}$ :  $[\text{M} + \text{H}] + m/z$ : 392.4814. Found: 392.4815. IR (KBr  $\text{cm}^{-1}$ ): 3019, 2479, 1647, 1480, 1330, 1160, 724, 582.

**(S)-6H-1-(5-Isoquinolinesulfonyl)-2-hydroxymethyl-1-pyrrolidine (compound 5).** Isoquinoline sulfonyl chloride hydrochloride (5 g, 18.9 mmol) was slowly added to a

saturated sodium bicarbonate solution (2.52 g, 30 mmol); the pH of the solution was kept at 5–6. The mixture was stirred 0.5 h and extracted with 20-mL  $\text{CH}_2\text{Cl}_2$ . The organic layers were dried and concentrated. The residue dissolved in 20-mL  $\text{CH}_2\text{Cl}_2$  was added dropwise to the flask containing D-prolinol (2.29 g, 22.6 mmol) and triethylamine (1.91 g, 18.9 mmol). The mixture was stirred at 0–5°C for 2 h. Then, it was concentrated, and the residue was dissolved in 50-mL ethyl acetate. The organic layer was washed with 20-mL water for three times. After dried and concentrated, the residue was purified by flash chromatography (ethyl acetate) to afford compound **5** (5.29 g, 95%) as a yellow oil.  $^1\text{H}$  NMR (400 MHz,  $\text{CDCl}_3$ )  $\delta$ : 9.42 (s, 1H), 8.74 (s, 2H), 8.49 (d,  $J = 7.3$  Hz, 1H), 8.29 (d,  $J = 8.1$  Hz, 1H), 7.78 (t,  $J = 7.8$  Hz, 1H), 3.97–3.82 (m, 1H), 3.71 (d,  $J = 11.4$  Hz, 2H), 3.56–3.32 (m, 2H), 1.99–1.70 (m, 3H), 1.66–1.51 (m, 1H).  $^{13}\text{C}$  NMR (100 MHz,  $\text{CDCl}_3$ )  $\delta$ : 25.27, 29.39, 50.44, 62.70, 65.04, 124.31, 130.13, 131.35, 134.52, 136.42, 136.71, 137.41, 139.97, 149.74. HRMS (ESI), Calcd  $\text{C}_{14}\text{H}_{16}\text{N}_2\text{O}_3\text{S}$ :  $[\text{M} + \text{H}] + m/z$ : 293.0957. Found: 293.0959. IR (KBr  $\text{cm}^{-1}$ ): 3600, 2580, 1720, 1318, 1161, 820, 580.

**(S)-6H-1-(5-Isoquinolinesulfonyl)-2-chloromethyl-1-pyrrolidine (compound 6).** Compound **5** (5 g, 0.02 mol) was added to thionyl chloride (20 mL, 0.27 mol), and the reaction mixture was stirred at 40°C for 8 h. And then, thionyl chloride was distilled. The sodium bicarbonate saturated aqueous solution was added to keep the pH of the solution (7–8). The residue was extracted with 60-mL  $\text{CH}_2\text{Cl}_2$ . The crude was purified by flash chromatography (ethyl acetate) to afford compound **6** (3.91 g, 75%) as a dense yellow oil.  $^1\text{H}$  NMR (400 MHz,  $\text{CD}_3\text{OD}$ ): 9.87 (s, 1H), 8.93 (d,  $J = 5.8$  Hz, 1H), 8.72 (s, 1H), 8.61 (d,  $J = 7.3$  Hz, 2H), 7.92 (t,  $J = 7.4$  Hz, 1H), 4.14 (s, 1H), 3.78 (d,  $J = 11$  Hz, 1H), 3.66–3.50 (m, 1H), 3.40 (d,  $J = 16.5$  Hz, 2H), 2.18–1.56 (m, 5H).  $^{13}\text{C}$  NMR (100 MHz,  $\text{CD}_3\text{OD}$ ): 25.12, 30.46, 47.69, 49.47, 50.87, 62, 124.20, 130.17, 131.45, 134.51, 136.13, 136.72, 137.68, 140.17, 149.80. HRMS (ESI), Calcd  $\text{C}_{15}\text{H}_{16}\text{ClNO}_2\text{S}$ :  $[\text{M} + \text{H}] + m/z$ : 311.0614. Found: 311.0615. IR: 3019, 2479, 1647, 1480, 1330, 1160, 729, 581.

## BIOLOGICAL METHODS

**ROCK activity.** ROCK activity was measured by the CycLex Research Product ROCK assay kit (CycLex Co., Ltd, Nagano, Japan). BV-2 microglia were treated with fasudil and the synthesized compounds (10  $\mu\text{g}/\text{mL}$ ) for 24 h and then homogenized on ice in four volumes of extraction buffer (pH 8.0, 0.1% triton X-100, 50-mM Tris-HCl, 1-mM EGTA, 1-mM ethylenediaminetetraacetic acid, 10-mM NaF, 0.5-mM PMSF, and 10-mM

betamercapto ethanol). Collecting the supernatants, BV-2 microglial cells were then centrifuged for 30 min at 12,000 revolutions per hour. Protein concentration was determined by a Bicinchoninic acid protein assay kit (Pierce) (CycLex Co., Ltd, Nagano, Japan). ROCK activity was then measured in 100  $\mu\text{L}$  of the supernatants (50-ng protein) as per the manufacturer's instructions. Optical density was measured at 490 nm.

**Observation of cell synapse.** BV-2 microglia were cultured as previously described and treated with fasudil and the synthesized compounds (15  $\mu\text{g}/\text{mL}$ ) for 24 h. Cells were fixed with 4% paraformaldehyde in 0.1-M phosphate-buffered saline (PBS) at room temperature for 20 min. BV-2 microglia were directly observed under a phase contrast microscope. Primary neurons were stained with anti-mouse monoclonal MAP-2 antibody at 4°C overnight. The cells were then washed with PBS and incubated with fluorescent-labeled secondary antibody at room temperature for 2 h. Cells were then sealed by 50% glycerol and observed under fluorescence microscope.

**Experimental autoimmune encephalomyelitis clinical symptoms. Preparation of the experimental autoimmune encephalomyelitis model mice cells.** According to the standard EAE model preparation program, immunized female C57BL/6 mice (8–10 weeks of age, 18–20 g) were purchased from Beijing Vital River Laboratory Animal Technology Co., Ltd. China. Prior to commencement of the experiment, the animals were housed in a clean, pathogen-free laboratory and had free access to a normal diet. After 1 week, the mice were randomly divided into nine groups: EAE control, abdominal injection fasudil, nasal cavity injection fasudil, and compounds **1** to **6** (15  $\mu\text{g}/\text{mL}$ ). The mean weight of the groups was equal. The animals were anesthetized using ether, and then, antigen emulsion 0.1 mL injected subcutaneously into the second half of the spine on both sides of the midline points. At 48 h after immunization (day 0), the groups of mice were injected with pertussis 800 mg as an immune enhancer. The nasal cavity groups received fasudil and the other compounds (10  $\mu\text{g}$ ) by nasal drip injection every 3 days, until after 27 days of immunization.

**Inflammatory cell infiltration.** Frozen microcomputer brain tissue was sliced at a thickness of 10  $\mu\text{M}$  in a frozen microtome. Before the measurement, the sections were taken out, dried at room temperature, and blocked with 1% bovine serum albumin for 1 h at room temperature. CD68 resistance in C57BL/6 mice incubated with the CD68 monoclonal antibody (1:400) at 4°C overnight. The next day, the tissue was washed with PBS, and fluorescein was added to mark rat IgG (1:1000) for an hour at room temperature. PBS was then used as a wash and 50% glycerol to seal prior to fluorescence microscopy examination.

**Acknowledgment.** The authors would like to acknowledge Professor Baoguo Xiao of Fudan University for the biological activity evaluations in this paper.

#### REFERENCES AND NOTES

- [1] Dias, D. S.; Fontes, L. A.; Crotti, A. M.; Aarestrup, B. V.; Aarestrup, F. M.; da Silva Filho, A. A.; Corrêa, J. A. *Molecules* 2014, 19, 12814.
- [2] Amano, M.; Fukata, Y.; Kaibuchi, K. *Exp Cell Res* 2000, 261, 44.
- [3] Rao, V. P.; Epstein, D. L. *BioDrugs* 2007, 21, 167.
- [4] Liao, J. K.; Seto, M.; Noma, K. *J. Cardiovasc Pharmacol* 2007, 50, 17.
- [5] Iwakubo, M.; Takami, A.; Okada, Y.; Kawata, T.; Tagami, Y.; Ohashi, H.; Sato, M.; Sugiyama, T.; Fukushima, K.; Taya, S.; Iijima, H. *Bioorg Med Chem* 2007, 15, 1022.
- [6] Iwakubo, M.; Takami, A.; Okada, Y.; Kawata, T.; Tagami, Y.; Ohashi, H.; Sato, M.; Sugiyama, T.; Fukushima, K.; Iijima, H. *Bioorg Med Chem* 2007, 15, 350.
- [7] Takami, A.; Iwakubo, M.; Okada, Y.; Kawata, T.; Odai, H.; Takahashi, N.; Shindo, K.; Kimura, K.; Tagami, Y.; Miyake, M.; Fukushima, K.; Inagaki, M.; Amano, M.; Kaibuchi, K.; Iijima, H. *Bioorg Med Chem* 2004, 12, 2115.
- [8] Shen, M. Y.; Yu, H. D.; Li, Y. Y.; Li, P. X.; Pan, P. C.; Zhou, S. Y.; Zhang, L. L.; Li, S.; Lee, S. M.; Hou, T. J. *Mol Biosyst* 2013, 9, 1511.
- [9] Tamura, M.; Nakao, H.; Yoshizaki, H.; Shiratsuchi, M.; Shigyo, H.; Yamada, H.; Ozawa, T.; Totsuka, J.; Hidaka, H. *Biochim Biophys Acta* 2005, 175, 245.
- [10] Chen, S.; Luo, M.; Zhao, Y.; Zhang, Y.; He, M. *Cell Physiol Biochem* 2015, 36, 531.
- [11] Yu, J. Z.; Chen, C.; Zhang, Q.; Zhao, Y.; Feng, L. *Wound Repair Regen* 2016, 24, 317.
- [12] Song, G. B.; Xi, G. P.; Li, Y. H.; Li, J. S.; Liu, J. C.; Chai, Z.; Xiao, B. G.; Zhang, G. X.; Ma, C. G. *Chin J Pathophysiol* 2017, 33, 2113.
- [13] Li, H.; Wang, D. H.; Liu, S.; Sun, C. H.; Chen, M. Z.; Wang, X. R.; Chen, L. G. *Pharm* 2014, 69, 1.
- [14] Kubo, T.; Hata, K.; Yamauchi, A. Yamashita, T. *Curr Pharm Des* 2007, 13, 2493.
- [15] Lingor, P.; Tonges, L.; Pieper, N.; Bermel, C.; Barski, E.; Planchamp, V.; Bahr, M. *Brain* 2008, 131, 250.
- [16] Lingor, P.; Teusch, N.; Schwarz, K.; Mueller, R.; Mack, H.; Bahr, M.; Mueller, B. K. *J. Neurochem* 2007, 103, 181.
- [17] Monnier, P. P.; Sierra, A.; Schwab, J. M.; Henke-Fahle, S.; Mueller, B. K. *Mol Cell Neurosci* 2003, 22, 319.
- [18] Wang, X. R.; Chen, L. G.; Li, H.; Sun, C. H.; Qi, H. F.; Wang, D. H. *J. Heterocyclic Chem* 2015, 52, 1212.
- [19] Hou, Y.; Zhou, L.; Yang, Q. D.; Du, X. P.; Li, M.; Yuan, M.; Zhou, Z. W. *Neuroscience* 2012, 200, 120.
- [20] Mueller, B. K.; Mack, H.; Teusch, N. *Nat Rev Drug Discov* 2005, 4, 387.
- [21] Noma, K.; Oyama, N.; Liao, J. K. *Am J Physiol Cell Physiol* 2006, 290, 661.
- [22] Zhang, H.; Zhang, H. F.; Li, Y. H.; Liu, C. Y.; Yu, J. Z.; Ding, Z. B.; Yang, X. W.; Yang, W. F.; Li, J. L.; Feng, Q. J.; Feng, L.; Xiao, B. G.; Ma, C. G. *J. Pathophysiol* 2013, 29, 2060.

#### SUPPORTING INFORMATION

Additional supporting information may be found online in the Supporting Information section at the end of the article.